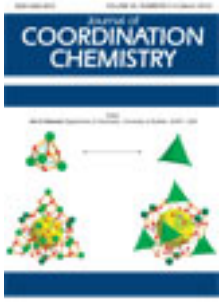

Journal of Coordination Chemistry
Publication details, including instructions for authors and subscription information:
http://www.tandfonline.com/loi/gcoo20

Synthesis, characterization, and biological activity of nickel(II) complexes with a tridentate Schiff base derived from heterocyclic aldehyde

R.N. Patel [a], Anurag Singh [a], Vishnu P. Sondhiya [a], Yogendra Singh [a], K.K. Shukla [a], D.K. Patel [a] & R. Pandey [a]
[a] Department of Chemistry, A.P.S. University, Rewa 486003, Madhya Pradesh, India
Published online: 16 Feb 2012.

To cite this article: R.N. Patel, Anurag Singh, Vishnu P. Sondhiya, Yogendra Singh, K.K. Shukla, D.K. Patel & R. Pandey (2012) Synthesis, characterization, and biological activity of nickel(II) complexes with a tridentate Schiff base derived from heterocyclic aldehyde, Journal of Coordination Chemistry, 65:5, 795-812, DOI: 10.1080/00958972.2012.662592

To link to this article: http://dx.doi.org/10.1080/00958972.2012.662592

Journal of Coordination Chemistry
Vol. 65, No. 5, 10 March 2012, 795–812

Synthesis, characterization, and biological activity of nickel(II) complexes with a tridentate Schiff base derived from heterocyclic aldehyde

R.N. PATEL*, ANURAG SINGH, VISHNU P. SONDHIYA, YOGENDRA SINGH, K.K. SHUKLA, D.K. PATEL and R. PANDEY

Department of Chemistry, A.P.S. University, Rewa 486003, Madhya Pradesh, India

(*Received 4 November 2011; in final form 2 January 2012*)

A series of nickel(II) complexes, namely $[Ni(L)_2]$ (**1**), $[Ni(L)(HL)](ClO_4)(H_2O)$ (**2**), $[Ni(HL)(bipy)(H_2O)](NO_3)(ClO_4)(H_2O)$ (**3**), and $[Ni(HL)(dien)](ClO_4)_2(H_2O)$ (**4**) have been synthesized with Schiff base (L) derived from 2-pyridinecarboxaldehyde and benzoylhydrazine. The elemental analyses of the complexes indicate stoichiometry ML_2 and M(L)(B), where L = N-[(1)-pyridin-2-ylmethylidene]benzohydrazide, B = diethylenetriamine/2,2′-bipyridine. L is a deprotonated as well as neutral tridentate ligand. Single-crystal X-ray structures of **1**–**4** reveal distorted octahedral geometry in the complexes. The molecules are connected by various hydrogen-bonding interactions. Magnetic susceptibility measurements at room temperature were 2.79–2.91 MB. The electrochemical behavior, superoxide dismutase, and antibacterial activities of these complexes were made by cyclic voltammetry, the alkaline DMSO-nitro blue tetrazolium chloride assay, and the paper disc diffusion method, respectively.

Keywords: Hydrogen bonds; Crystal engineering; Cyclic voltammetry

1. Introduction

Schiff bases have roles in biological systems [1, 2] as models to evaluate activity of proteins [3]. The features of these compounds are their preparative accessibility, diversity, and structural variability, which make them very attractive. Many papers indicate that the environment around the metal and the conformational flexibility of the ligands are important because they allow metalloproteins to carry out a specific biological function. For example, the flexibility of the ethylenediamine backbone in salen is the main structural feature for oxygen activation [4]. The construction of supramolecular architecture [5–8] through selective and directional non-covalent forces such as hydrogen-bonding [9–11], $\pi\cdots\pi$ [12], and C–H$\cdots\pi$ [13, 14] interactions in metallo-organic frameworks are of considerable interest due to their potential applications as functional materials [15–19]. Other co-workers are also active in this field [9, 20–23] through variation of ligand backbones and metal ion coordination environments.

*Corresponding author. Email: rnp64@ymail.com

ISSN 0095-8972 print/ISSN 1029-0389 online
http://dx.doi.org/10.1080/00958972.2012.662592

2,2′-Bipyridine may form $\pi\cdots\pi$ and C–H$\cdots\pi$ interactions through pyridyl planes, leading to different crystalline aggregates [24–29].

Considerable attention has been paid to pyridine and related N-containing heterocyclic derivatives [30]. We have synthesized a tridentate ligand (N-[(1)-pyridin-2-ylmethylidene]benzohydrazide) carrying C=N bond and its complexes with nickel(II) namely $[Ni(L)_2]$ (**1**), $[Ni(L)(HL)](ClO_4)(H_2O)$ (**2**), $[Ni(HL)(bipy)(H_2O)](NO_3)(ClO_4)(H_2O)$ (**3**), and $[Ni(HL)(dien)](ClO_4)_2(H_2O)$ (**4**). Biological activities have been investigated by alkaline DMSO-nitro blue tetrazolium chloride (NBT) assay.

2. Experimental

2.1. *Materials*

Nickel(II) nitrate hexahydrate was purchased from S.D. fine-chemicals, India. All other chemicals used were of synthetic grade and used without purification.

2.2. *Physical measurements*

2.2.1. Elemental and FAB mass analysis. Elemental analyses were performed on an Elementar Vario EL III Carlo Erba 1108 analyser. Fast atomic bombardment (FAB) mass spectra were recorded on a JEOL SX 102/DA 6000 Mass Spectrometer using xenon (6 kV, 10 mA) as the FAB gas. The accelerating voltage was 10 kV and the spectra were recorded at room temperature.

2.2.2. Spectroscopy. UV-Vis spectra were recorded at 298 K on a Shimadzu UV-Vis recording Spectrophotometer UV-160 in quartz cells. Infrared (IR) spectra were recorded in KBr on a Perkin-Elmer spectrophotometer.

2.2.3. Electrochemistry. Cyclic voltammetry was carried out on solutions containing 0.1 mol L^{-1} $NaClO_4$ with a BAS-100 Epsilon electrochemical analyzer having an electrochemical cell with a three-electrode configuration. Ag/AgCl was used as a reference electrode, glassy carbon as working electrode, and platinum wire as an auxiliary electrode. All measurements were carried out at 298 K under nitrogen. Molar conductivities of freshly prepared 2×10^{-3} mol L^{-1} of DMSO solutions were measured on a Systronics conductivity TDS meter 308.

2.2.4. Magnetic susceptibility. Room temperature magnetic susceptibilities were measured by a Gouy balance using mercury(II) tetrathiocynato cobaltate(II) as calibrating agent ($\chi_g = 16.44 \times 10^{-6}$ c.g.s. units).

2.2.5. SOD activity. The *in vitro* superoxide dismutase (SOD) activity was measured using alkaline DMSO as a source of superoxide radical (O_2^-) and NBT as O_2^- scavenger [31]. In general, 400 μL sample to be assayed was added to a solution

containing 2.1 mL of 0.2 mol L^{-1} potassium phosphate buffer (pH 8.6) and 1 mL of 56 μmol L^{-1} alkaline DMSO solution was added while stirring. The absorbance was then monitored at 540 nm against a sample prepared under similar conditions except NaOH in DMSO. A unit of SOD activity is the concentration of complex, which causes 50% inhibition of alkaline DMSO mediated reduction of NBT.

2.2.6. Antibacterial activity measurements. The *in-vitro* antibacterial activities of these complexes were tested using the paper disc diffusion method [32]. Autoclaved (20 min at 121°C and at 15 lb pressure) nutrient agar medium was poured into a sterile petri disc and allowed to solidify. Petri-dishes were seeded with bacterial species. Paper disc was placed at the dish after dipping test compound (DMSO solution). The width of the growth inhibition zone around the disc was measured after 24 h incubation at 37°C.

2.3. *Synthesis*

2.3.1. Synthesis of L/HL. The Schiff base was prepared by condensation of 2-pyridinecarboxaldehyde and benzoylhydrazine. A solution of 2-pyridinecarboxaldehyde (1.07 g, 10.0 mmol) in 10 mL ethanol was refluxed with an ethanolic solution of benzoylhydrazine (1.36 g, 10.0 mmol) continuously for 6 h. After some time 1–2 drops of acetic acid was added. On cooling the solution at room temperature pale yellow crystals were separated which were filtered and washed with methanol. These were dried in air at room temperature and stored in a $CaCl_2$ desiccator. Anal. Calcd for $C_{13}H_{11}N_3O$ (%): C, 69.32; H, 4.92; N, 18.66. Found (%): C, 69.02; H, 4.56; N, 18.45 (scheme 1).

2.3.2. Synthesis of [Ni(L)$_2$] (1). To an MeOH solution (10 mL) of $Ni(NO_3)_2 \cdot 6H_2O$ (0.29 g, 1.0 mmol) an MeOH solution (10 mL) of L (0.45 g, 2 mmol) was added. The resulting solution continued to stir for 30 min. After completion of reaction clear green solution was obtained. The resultant clear solution was filtered and left for slow evaporation. After 3–4 days light green crystals were collected which were suitable for X-ray crystallography and washed with MeOH and diethyl ether. These were dried in air at room temperature and stored in a $CaCl_2$ desiccator. Anal. Calcd for $C_{26}H_{20}NiN_6O_2$ (%): C, 61.51; H, 3.94; N, 16.56. Found (%): C, 60.85; H, 3.86; N, 16.12.

2.3.3. Synthesis of [Ni(L)(HL)](ClO$_4$)(H$_2$O) (2). Complex **2** was synthesized following the same procedure as **1**, only $NaClO_4$ (0.12 g, 1.0 mmol) was added to maintain the neutrality of the complex. Slow evaporation of reaction mixture afforded **2** as dark green crystals. Anal. Calcd for $C_{26}H_{21}ClNiN_6O_7$ (%): C, 50.02; H, 3.36; N, 13.47. Found (%): C, 51.22; H, 3.42; N, 13.89.

2.3.4. Synthesis of [Ni(HL)(bipy)(H$_2$O)](NO$_3$)(ClO$_4$)(H$_2$O) (3). To a stirred solution of $Ni(NO_3)_2 \cdot 6H_2O$ (0.29 g, 1.0 mmol) in MeOH (10 mL) was added L (1 mmol, 0.23 g) in MeOH (10 mL) at room temperature. The resulting solution continued to stir for 30 min and then bipy (0.16 g, 1 mmol) was added and stirred again for 45 min at

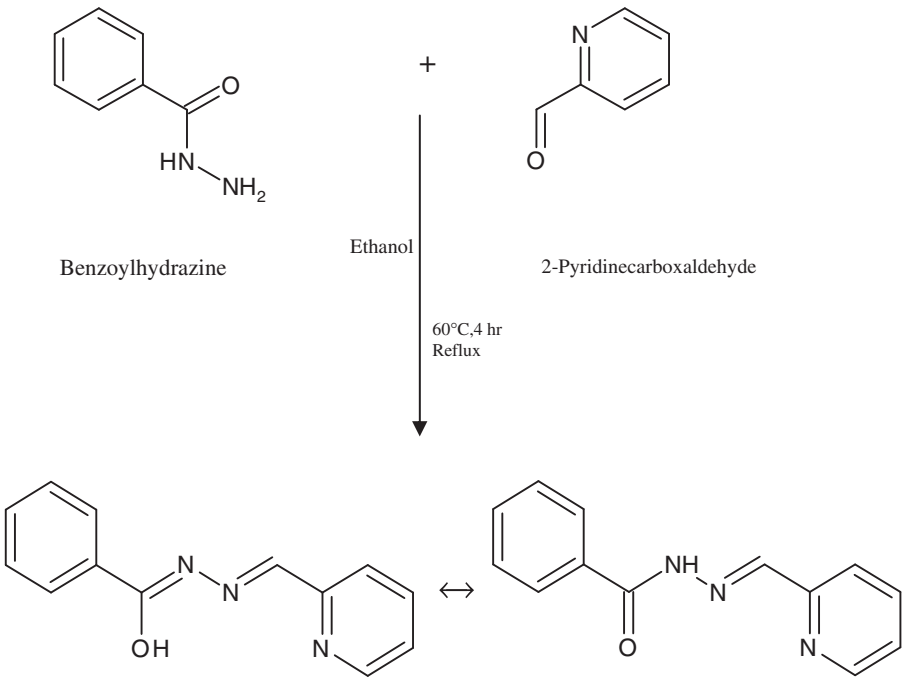

HL/L (2-[(1)-pyridin-2-ylmethylidene]benzohydrazide)

Scheme 1. Synthesis of ligand.

room temperature. After this $NaClO_4$ (0.12 g, 1 mmol) was added. The green product obtained was washed with methanol, dried in air, and stored in a $CaCl_2$ desiccator. Anal. Calcd for $C_{23}H_{23}ClNiN_6O_6$ (%): C, 43.28; H, 3.60; N, 13.17. Found (%): C, 43.11; H, 3.42; N, 13.01.

2.3.5. Synthesis of [Ni(HL)(dien)]$(ClO_4)_2(H_2O)$ (4). Complex **4** was synthesized in a similar way as **3** by using dien (0.95 g, 1 mmol) and $NaClO_4$ (0.24 g, 2.0 mmol). Slow evaporation of reaction mixture afforded **4** as a dark green crystal. Anal. Calcd for $C_{17}H_{26}Cl_2NiN_6O_{10}$ (%): C, 33.77; H, 4.30; N, 13.90. Found (%): C, 33.16; H, 3.65; N, 13.68 (synthesis of complexes are presented in scheme 2).

2.3.6. Crystal structure determination. Crystals suitable for single-crystal X-ray analysis of all complexes were grown by slow evaporation of the reaction mixtures at room temperature. Single-crystals suitable for single-crystal X-ray analysis were mounted on glass fibers and used for data collection. Crystal data were collected on an Enraf-Nonius $MACH_3$ diffractometer using graphite monochromated Mo-Kα radiation ($\lambda = 0.71073$ Å). The crystal orientation, cell refinement, and intensity measurements were made using CAD-4PC performing ψ-scan measurements. The structures were solved by direct methods using SHELXS-97 [33] and refined by

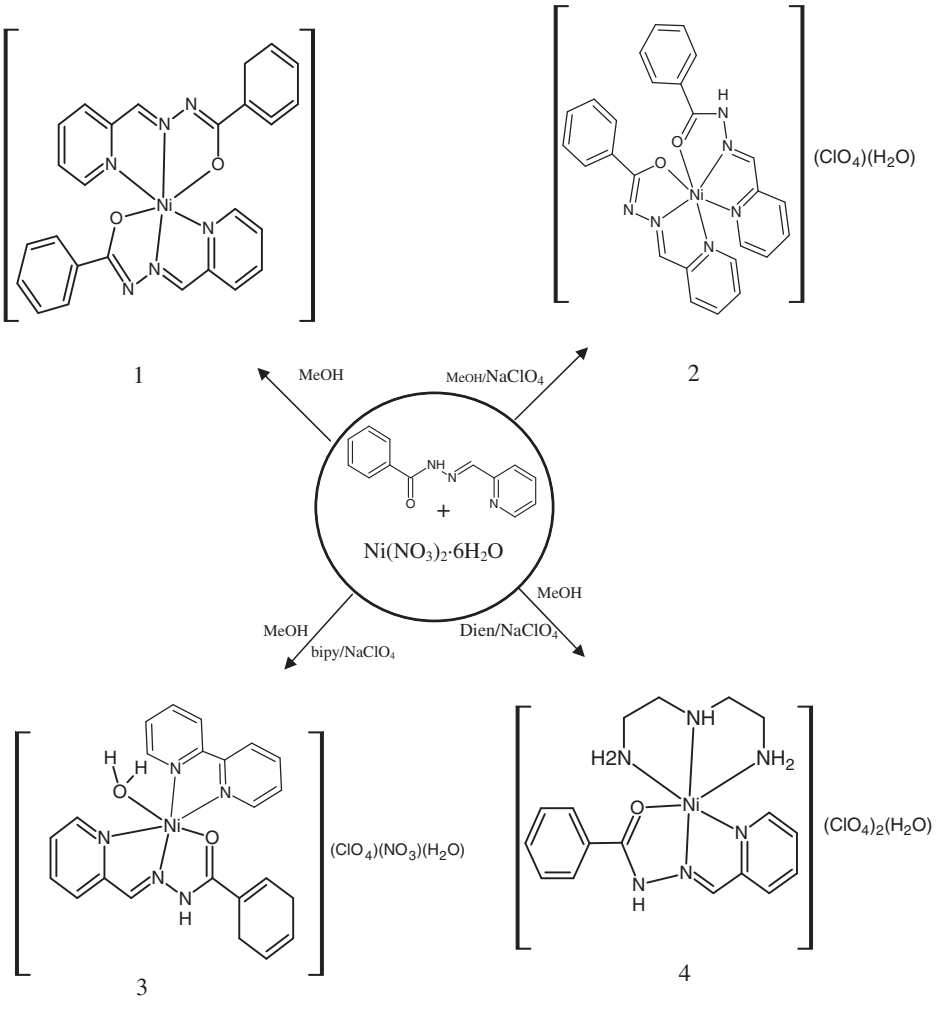

Scheme 2. Synthesis of **1–4**.

full-matrix least-squares against F^2 using SHELXL-97 [34]. All non-hydrogen atoms were refined anisotropically. All hydrogen atoms were geometrically fixed and allowed to refine using a riding model.

3. Results and discussion

3.1. *Synthesis of complexes*

Condensation of 2-pyridinecarboxaldehyde and benzoyl hydrazine in a 1 : 1 molar ratio yields Schiff bases which further react with nickel nitrate hexahydrate to yield the

corresponding 2 : 1 nickel(II) complexes **1** and **2**. Further reaction of these starting materials with bipy and dien in 1 : 1 molar ratio yielded **3** and **4**. Stoichiometric amounts of nickel(II) salts and ligand were dissolved separately in corresponding solvents and resulting solutions were mixed. In most cases, the product precipitated immediately and the mixture was left overnight. The product was washed, dried in air, and stored in a $CaCl_2$ desiccator.

The obtained crystalline nickel(II) complexes **1**, **2**, **3**, and **4** are stable in air and soluble in coordinating solvents such as DMF and DMSO, slightly soluble in ethanol and insoluble in water and most of organic solvents.

3.2. *Crystal structures of the complexes*

X-ray measurements of the four nickel complexes were made at 298 K using suitable crystal for data collection. Crystallographic data and structure refinement parameters are given in table 1. The relevant bond lengths and angles are listed in tables 2–5.

3.2.1. $[Ni(L)_2]$ (1) and $[Ni(L)(HL)](ClO_4)(H_2O)$ (2). Single-crystal X-ray analysis of **1** and **2** revealed that both complexes crystallized in the monoclinic space group $P2_1/n$ with four molecules in the unit cell. The ORTEP representations of the complexes are illustrated in figures 1 and 2. In **1** and **2** L uses NNO for coordination to nickel(II), leading to 2 : 1 stoichiometry in a monomer. The ligand in **1** and **2** is deprotonated

Table 1. Crystal refinement parameters of **1–4**.

Parameters	1	2	3	4
Empirical formula	$C_{26}H_{20}N_6NiO_2$	$C_{26}H_{21}ClN_6NiO_7$	$C_{23}H_{23}ClN_6NiO_{10}$	$C_{17}H_{26}Cl_2N_6NiO_{10}$
Formula weight	507.19	623.23	637.63	604.05
Temperature (K)	150(2)	150(2)	150(2)	120(2)
Crystal system	Monoclinic	Monoclinic	Orthorhombic	Monoclinic
Space group	$P2_1/n$	$P2_1/c$	$Pna2_1$	$P2_1/n$
Unit cell dimensions (Å, °)				
a	9.6576(4)	11.358(5)	12.2740(2)	14.1586(3)
b	23.8274(8)	23.799(5)	17.6746(3)	11.2278(2)
c	10.2719(3)	10.357(5)	12.2291(2)	15.7494(3)
α	90	90	90	90
β	105.193(4)	105.262(5)	90	105.370(2)
γ	90	90	90	90
Volume (Å^3), Z	2281.11(14), 4	2700.9(19), 4	2652.96(8), 4	2414.13(8), 4
Calculated density (Mg m^{-3})	1.477	1.534	1.596	1.662
Crystal size (mm^3)	0.23 × 0.18 × 0.13	0.28 × 0.24 × 0.22	0.23 × 0.18 × 0.13	0.23 × 0.18 × 0.14
θ range for data collection (°)	3.09–25.00	3.2–25.00	3.29–25.00	2.98–25.00
Reflections collected	17,386	19,648	17,771	17,573
Data/restraint/parameters	4011/0/316	4706/0/374	4240/1/390	4250/0/357
Goodness-of-fit on F^2	0.992	0.960	1.015	1.067
Final R indices [$I > 2\sigma(I)$]	$R_1 = 0.0271$, $wR_2 = 0.0679$	$R_1 = 0.0627$, $wR_2 = 0.1833$	$R_1 = 0.0260$, $wR_2 = 0.0648$	$R_1 = 0.0275$, $wR_2 = 0.0793$
R indices (all data)	$R_1 = 0.0373$, $wR_2 = 0.0696$	$R_1 = 0.0789$, $wR_2 = 0.1838$	$R_1 = 0.0292$, $wR_2 = 0.0657$	$R_1 = 0.0331$, $wR_2 = 0.0810$

Table 2. Selected bond lengths (Å) and angles (°) for **1**.

Ni(1)–N(2)	1.979(14)	N(5)–N(6)	1.362(2)
Ni(1)–N(5)	1.987(14)	N(6)–C(20)	1.339(2)
Ni(1)–O(2)	2.098(13)	N(2)–C(6)	1.275(2)
Ni(1)–N(1)	2.128(15)	N(2)–N(3)	1.366(2)
Ni(1)–N(4)	2.129(16)	N(3)–C(7)	1.335(2)
Ni(1)–O(1)	2.133(13)	N(2)–N(3)	1.366(2)
O(1)–C(7)	1.267(2)	O(2)–C(20)	1.267(2)
N(2)–Ni(1)–N(5)	173.24(6)	N(5)–Ni(1)–O(1)	110.57(5)
N(2)–Ni(1)–O(2)	106.35(5)	O(2)–Ni(1)–O(1)	95.90(5)
N(5)–Ni(1)–O(2)	76.20(5)	N(1)–Ni(1)–O(1)	153.49(5)
N(2)–Ni(1)–N(1)	77.92(6)	N(4)–Ni(1)–O(1)	88.77(6)
N(5)–Ni(1)–N(1)	95.94(6)	N(3)–N(2)–Ni(1)	120.15(12)
O(2)–Ni(1)–N(1)	90.00(5)	N(1)–Ni(1)–N(4)	97.32(6)
N(2)–Ni(1)–N(4)	99.92(6)	N(2)–Ni(1)–O(1)	75.61(6)
N(5)–Ni(1)–N(4)	77.89(6)	N(6)–N(5)–Ni(1)	118.74(11)
O(2)–Ni(1)–N(4)	153.66(5)		

Table 3. Selected bond lengths (Å) and angles (°) for **2**.

Ni(1)–N(5)	1.954(4)	N(2)–C(7)	1.340(6)
Ni(1)–N(3)	1.997(3)	N(2)–N(3)	1.371(5)
Ni(1)–N(1)	2.087(4)	N(3)–C(6)	1.266(5)
Ni(1)–N(4)	2.089(4)	N(5)–N(6)	1.375(5)
Ni(1)–O(2)	2.116(3)	N(6)–C(20)	1.320(6)
Ni(1)–O(1)	2.182(4)	O(2)–C(20)	1.296(5)
O(1)–C(7)	1.244(5)	C(19)–N(5)	1.282(6)
N(5)–Ni(1)–N(3)	177.24(15)	N(4)–Ni(1)–O(1)	89.39(13)
N(5)–Ni(1)–N(1)	100.31(15)	O(2)–Ni(1)–O(1)	95.68(12)
N(3)–Ni(1)–N(1)	77.58(14)	N(2)–N(3)–Ni(1)	117.3(3)
N(5)–Ni(1)–N(4)	79.18(15)	N(1)–Ni(1)–O(2)	90.51(13)
N(3)–Ni(1)–N(4)	99.20(15)	N(4)–Ni(1)–O(2)	155.41(14)
N(1)–Ni(1)–N(4)	96.12(14)	N(5)–Ni(1)–O(1)	107.39(14)
N(5)–Ni(1)–O(2)	76.34(14)	N(3)–Ni(1)–O(1)	74.74(13)
N(3)–Ni(1)–O(2)	105.35(13)	N(1)–Ni(1)–O(1)	152.30(13)

Table 4. Selected bond lengths (Å) and angles (°) for **3**.

Ni(1)–N(4)	1.998(19)	N(4)–C(16)	1.282(4)
Ni(1)–N(1)	2.025(2)	N(4)–N(5)	1.360(3)
Ni(1)–N(2)	2.047(2)	N(5)–C(17)	1.356(3)
Ni(1)–O(101)	2.063(2)	Ni(1)–O(1)	2.153(18)
Ni(1)–N(3)	2.098(2)		
N(4)–Ni(1)–N(1)	178.05(8)	N(2)–Ni(1)–O(1)	90.09(8)
N(4)–Ni(1)–N(2)	98.77(9)	O(101)–Ni(1)–O(1)	87.66(8)
N(1)–Ni(1)–N(2)	79.82(9)	N(3)–Ni(1)–O(1)	153.77(8)
N(4)–Ni(1)–O(101)	88.46(8)	N(5)–N(4)–Ni(1)	116.05(17)
N(1)–Ni(1)–O(101)	93.04(9)	N(2)–Ni(1)–N(3)	91.74(8)
N(2)–Ni(1)–O(101)	171.69(8)	O(101)–Ni(1)–N(3)	93.82(9)
N(4)–Ni(1)–N(3)	77.62(9)	N(4)–Ni(1)–O(1)	76.25(9)
N(1)–Ni(1)–N(3)	101.04(9)	N(1)–Ni(1)–O(1)	105.04(8)

Table 5. Selected bond lengths (Å) and angles (°) for **4**.

Ni(1)–N(2)	2.013(18)	Ni(1)–N(6)	2.093(2)
Ni(1)–N(5)	2.062(19)	N(2)–N(3)	1.357(3)
Ni(1)–N(4)	2.090(2)	N(3)–C(7)	1.362(3)
Ni(1)–N(1)	2.119(18)	N(2)–N(3)	1.357(3)
N(2)–C(6)	1.280(3)		
N(2)–Ni(1)–N(5)	177.82(8)	N(6)–Ni(1)–O(1)	87.01(7)
N(2)–Ni(1)–N(4)	98.13(7)	N(1)–Ni(1)–O(1)	152.15(6)
N(5)–Ni(1)–N(4)	82.63(7)	N(3)–N(2)–Ni(1)	117.43(13)
N(2)–Ni(1)–N(6)	96.16(7)	N(4)–Ni(1)–N(1)	94.56(8)
N(5)–Ni(1)–N(6)	82.72(8)	N(6)–Ni(1)–N(1)	99.23(8)
N(4)–Ni(1)–N(6)	161.95(8)	N(2)–Ni(1)–O(1)	74.65(6)
N(2)–Ni(1)–N(1)	77.69(7)	N(5)–Ni(1)–O(1)	103.39(7)
N(5)–Ni(1)–N(1)	104.31(8)	N(4)–Ni(1)–O(1)	86.19(8)

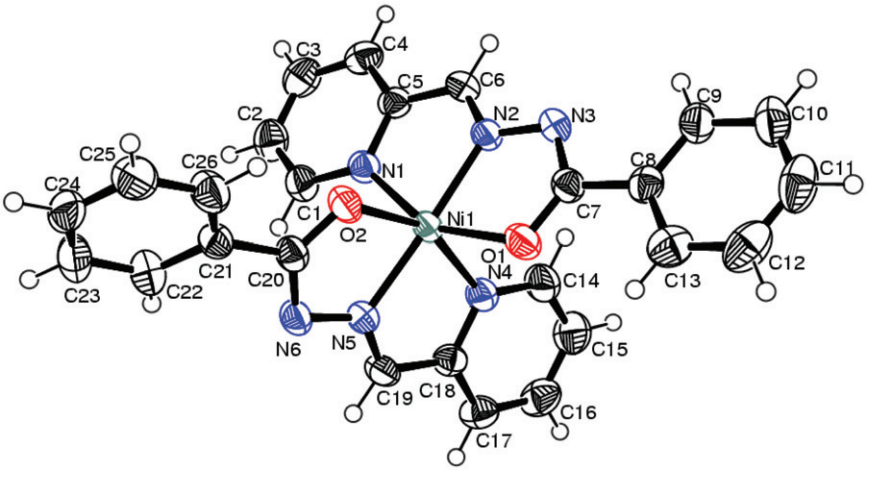

Figure 1. ORTEP view of **1**.

mononegative N_2O tridentate, coordinating *via* its enolic oxygen, azomethine nitrogen, and pyridine nitrogen, giving a distorted octahedral geometry around nickel. Such molecule can be deprotonated in the presence of metal ion [34] and can undergo complexation with metal in neutral media. Protonated ligand can also undergo similar reaction with metals. In **1** both ligands are deprotonated while in **2** only one molecule is deprotonated; in both cases they coordinate meridional [35] using pairs of pyridine nitrogen atoms, *trans* azomethine nitrogen atoms, and *cis* carbonyl oxygen atoms. The apical positions are occupied by pyridine nitrogen atom and carbonyl oxygen atom, completing the coordination sphere. The C–N bond lengths C(19)–N(5) = 1.282 and C(6)–N(2) = 1.275 Å for **1** and C(19)–N(5) = 1.282(6) and C(6)–N(3) = 1.266(5) Å for **2** are consistent with partial double bond character. These factors confirm coordination through the enolate form by deprotonation after enolization of the ligand. Selected bond lengths and angles within **1** and **2** are listed in tables 2 and 3. The values obtained in this study are comparable with those obtained previously [36]. However, the mutual disposition of the ligands deviates noticeable from perpendicularly which is indicated by

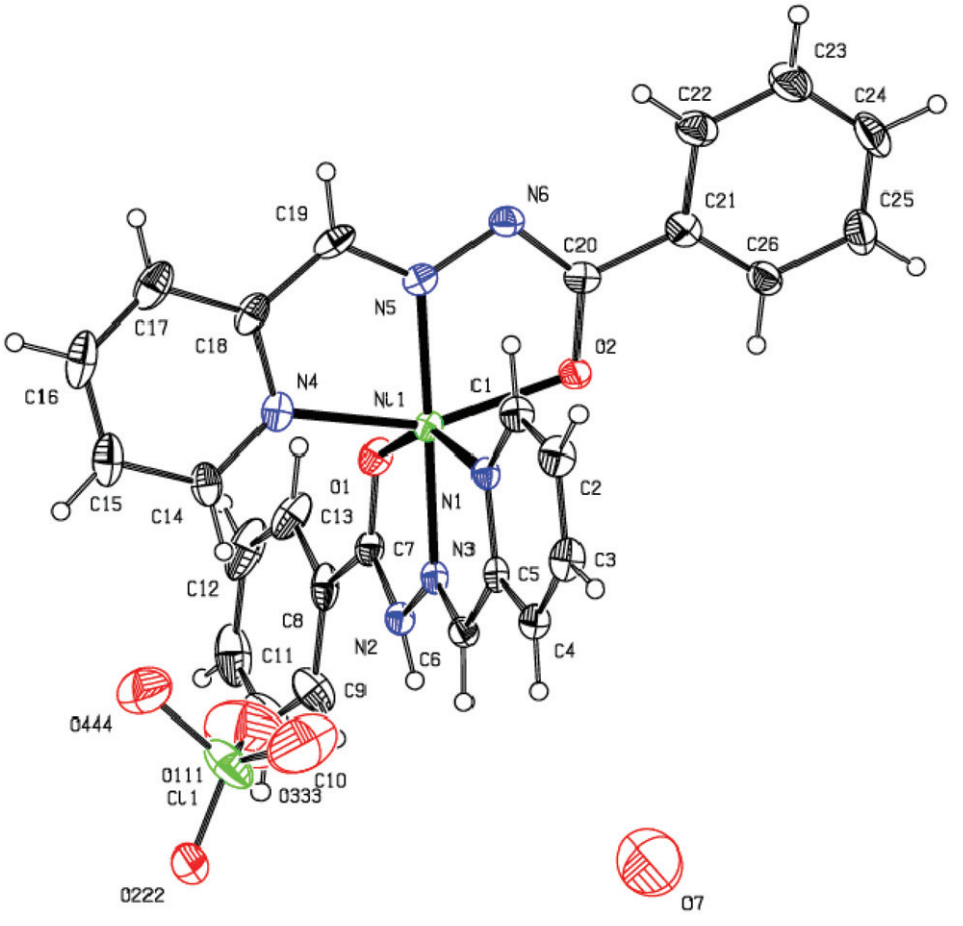

Figure 2. ORTEP view of **2**.

decreased values of the *trans* angles, N(1)–Ni–O(1) = 153.49(5)°, N(4)–N–O(2) = 153.66(5)°, and N(2)–Ni–N(5) = 173.24(6)° for **1** and N(5)–Ni–N(3) = 177.24(15)°, N(4)–Ni–O(2) = 155.41(14)°, and N(1)–Ni–O(1) = 152.30(13)° for **2**. Bond distances between the donor and metal are Ni–N(2) = 1.9795(4), Ni–N(5) = 1.9866(14), Ni–O(2) = 2.0979(1), Ni–N(4) = 2.1286(6), Ni–O(1) = 2.1332(13), and Ni–N(1) = 2.1380(15) Å for **1** and Ni(1)–N(5) = 1.954(4), Ni(1)–N(3) = 1.997(3), Ni(1)–N(1) = 2.087(4), Ni(1)–N(4) = 2.089(4), Ni(1)–O(2) = 2.116(3), and Ni(1)–O(1) = 2.182(4) Å for **2**. Individual mean bond distances and angles within the coordination polyhedra compare well with those found in other octahedral complexes of nickel(II) involving N donors [37]. The *cisoid* and *transoid* angles reflect the degree of distortion from ideal octahedral geometry.

Each ligand in both complexes forms two planar chelate rings and dihedral angles. The dihedral angle between the pyridyl and chelate best planes is 78.93° for **1** and 84.72(0.13)° for **2** suggesting non co-planarity of the tridentate ligands which favors substantial electron delocalization over the ligand backbone.

3.2.2. [Ni(HL)(bipy)(H_2O)](NO_3)(ClO_4)(H_2O) (3) and [Ni(HL)(dien)](ClO_4)$_2$(H_2O) (4). Single crystal of **3** revealed that the complex belongs to the orthorhombic space group $Pna2_1$ with four molecules in the unit cell. The ORTEP representation is illustrated in figure 3. Water is present in the coordination sphere as well as in the crystal. Nickel(II) has N_4O_2 coordination with distorted octahedral geometry. Two neutral tridentate ligands are coordinated to the metal center meridional [35], similar to **1** and **2**, creating adjacent five-membered chelate rings. The C(16)–N(4) bond distance of 1.282(4) Å close to the theoretical predicted value of a double bond C=N (1.28 Å) [38] confirms formation of Schiff base [39]. Selected bond lengths and angles within the complex are listed in table 4. The distortion of the molecule is indicated by decreased values of the *trans* angles, N(4)–Ni–N(1) = 178.05(8)°, N(3)–Ni–O(1) = 153.77(8)°, and N(2)–Ni–O(101) = 171.69(8)°. The bond distances between donors and metal in the complex are Ni(1)–N(4) = 1.998(19), Ni(1)–N(1) = 2.025(2), Ni(1)–N(2) = 2.047(2), Ni(1)–O(101) = 2.063(2), Ni(1)–N(3) = 2.098(2), and Ni(1)–O(1) = 2.153(18) Å. The ketonic oxygen and nickel bond length is long compared to the aqua nickel bond, showing weak ketonic oxygen–nickel bond.

Single crystal of **4** revealed that the complex crystallized as green crystal that belongs to the monoclinic space group $P2_1/n$ with four molecules in the unit cell. The ORTEP representation of the complex is illustrated in figure 4. Complex **4** has N_5O

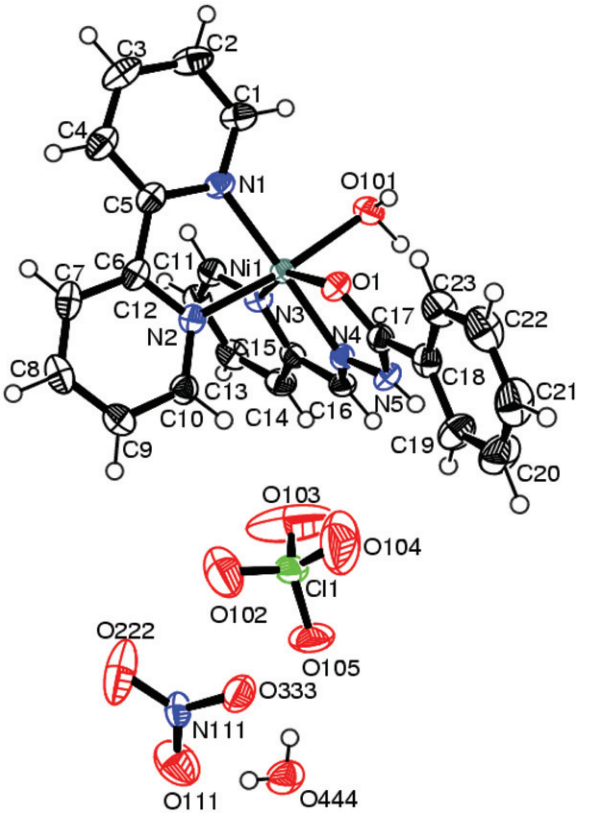

Figure 3. ORTEP view of **3**.

coordination and distorted octahedral geometry. Selected bond lengths and angles within the complex are listed in table 5. The values are comparable with those obtained previously in **1**, **2**, and **3**. Distortion from the octahedral geometry is evidenced by decreased values of the *trans* angles, N(2)–Ni–N(5) = 177.82(8)°, N(1)–Ni–O(1) = 152.15(6)°, and N(4)–Ni–N(6) = 161.95(8)°. The *cisoid* and *transoid* angles reflect the degree of distortion from ideal octahedral geometry.

The bond distances between donors and metal in **4** are Ni(1)–N(2) = 2.0130(18), Ni(1)–N(5) = 2.0619(19), Ni(1)–N(4) = 2.090(2), Ni(1)–N(6) = 2.093(2), Ni(1)–N(1) = 2.1188(8), and Ni(1)–O(1) = 2.2031(16) Å. Individual mean bond distances and angles within the coordination polyhedron compare well with those found in other octahedral complexes of nickel(II) involving N donors [37].

3.3. *Lattice structure and hydrogen-bonding*

All the complexes (except **1**, which shows only intramolecular H-bonding) are connected by various hydrogen-bonding interactions including water and anion wherever present. All four complexes show a clear C–H···anion hydrogen bond (table 6). In **2**, **3**, and **4** which have ClO_4^- the intermolecular H-bonds are formed by amine C–H donor/O–H donor/N–H donor and one anion with distance of 3.299, 2.794, and 2.935 Å for **2**, **3**, and **4**, respectively. The nitrate (**3**) also gives a similar

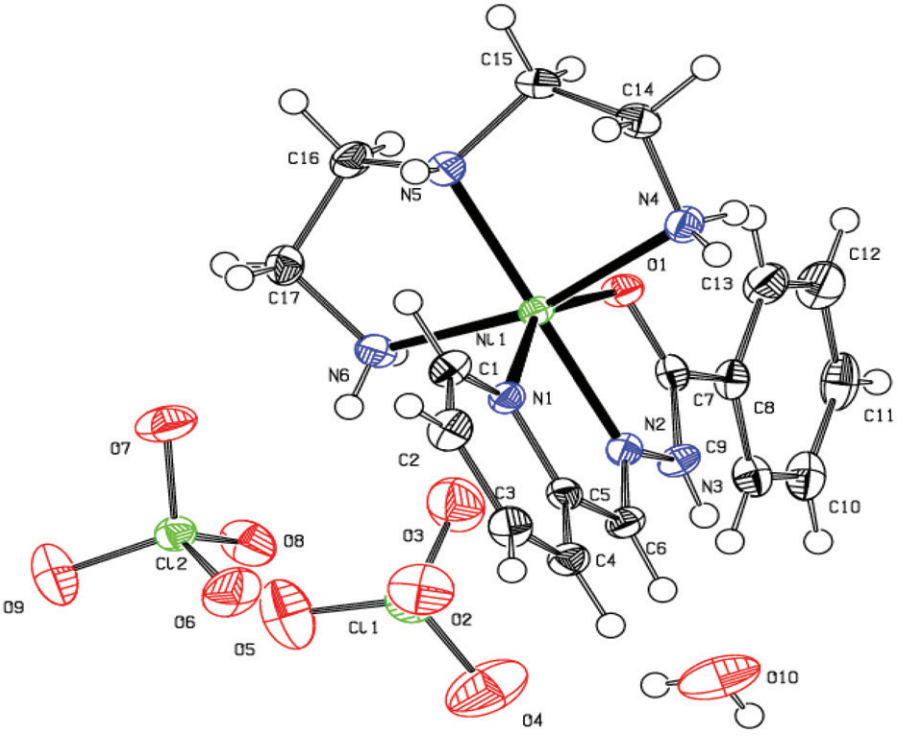

Figure 4. ORTEP view of **4**.

Table 6. Hydrogen-bonding interactions (Å and °) for **1**–**4**.

D–H···A		D–H (Å)	H···A (Å)	D···A (Å)	∠D–H···A (°)	Symmetry
Intramolecular						
2						
N2–H2N···O2	(2)	0.807(4)	1.91(4)	2.703(15)	152.0(4)	$-x+1,-y,-z+1$
3						
O101–H101···N4	(0)	1.014(0.054)	2.513(0.048)	2.834(0.003)	97.70(3.23)	x, y, z
O101–H101···O1	(0)	0.711(0.036)	2.763(0.036)	2.920(0.003)	95.70(3.11)	x, y, z
4						
N4–H4NA···O1	(0)	0.866(0.030)	2.592(0.026)	2.934(0.003)	104.74(1.93)	x, y, z
N4–H4NB···N1	(0)	0.789(0.030)	2.952(0.025)	3.092(0.003)	92.76(2.16)	x, y, z
N6–H6NA···O1	(0)	0.894(0.032)	2.625(0.025)	2.959(0.003)	103.16(2.12)	x, y, z
N4–H4NA···O2	(0)	0.894(0.032)	2.979(0.026)	3.105(0.003)	89.67(1.79)	x, y, z
N6–H6NA···O8	(0)	0.791(0.028)	2.338(0.030)	3.108(0.003)	164.93(2.92)	x, y, z
Intermolecular						
3						
O444–H111···O105	(0)	0.712(0.037)	2.083(0.037)	2.794(0.004)	176.90(4.00)	x, y, z
O444–H222···O111	(0)	0.877(0.057)	1.999(0.057)	2.857(0.004)	165.48(5.27)	x, y, z
4						
O10–H111···O4	(0)	0.803(0.026)	2.136(0.026)	2.935(0.003)	173.63(2.69)	x, y, z
N3–H3N···O10	(0)	0.780(0.027)	2.055(0.026)	2.800(0.003)	159.76(2.69)	x, y, z
N5–H5N···O7	(1)	0.739(0.028)	2.459(0.026)	3.138(0.003)	153.45(2.58)	$-x+1,-y+1,-z+2$
O10–H222···O3	(3)	0.709(0.055)	2.349(0.055)	3.005(0.004)	154.63(5.38)	$-x+1/2, y-1/2,-z+1/2+2$

Table 7. Absorption maxima, D_q, β, B, and β° of the octahedral nickel(II) complexes (ν_{max} in cm^{-1}).

Complex	$^3A_{2g}\rightarrow{}^3T_{2g}(\nu_1)$	$^3A_{2g}\rightarrow{}^3T_{1g}(F)(\nu_2)$	$^3A_{2g}\rightarrow{}^3T_{1g}(P)(\nu_3)$	ν_2/ν_1	D_q	β	B (cm^{-1})	β°
1	11,628	16,667	28,256, 33,333	1.43	1162	0.32	336	68
2	11,765	17,857	25,840, 33,333	1.50	1176	0.54	560	46
3	10,989	15,385	25,840, 33,333	1.40	1099	0.53	550	47
4	–	–	25,317, 33,898	–	–	–	–	–

15 $B=(\nu_2+\nu_3)-3\nu_1$; $\beta=B/B_0$ [B_0(free ion) = 1030]; $\beta^\circ=(1-\beta)\times 100$.

polymeric array. In the lattice, water with nitrate oxygen has strong (2.857(0.004) Å) intermolecular hydrogen-bonding interaction. The shortest contacts with any intermolecular atom are 4.0 Å [40].

3.4. *Electronic spectra*

Electronic spectral data for **1**–**4** are summarized in table 7. The spectra recorded in DMSO (3×10^{-3} mol L^{-1}) display several electronic transitions. In all the complexes strong peak (260 nm) at the blue end of the spectra can be ascribed to $\pi\cdots\pi^*$ pyridine ring absorption [41]. Due to increased conjugation in the complexes, it is shifted by 10–20 nm higher compared to the ligand. The paramagnetic nickel(II) complexes are characterized by two main bands at 300 and 400 nm, present in **1**–**3**. The band at 300 nm is $\pi\cdots\pi^*$ imine and $n\cdots\pi^*$ of both the imine and pyridine ring, which are also present in spectra of the

Table 8. IR spectroscopic assignments for ligand and **1**–**4**.

Complex	(C=N_{azo}) cm^{-1}	(C=^{2}N) cm^{-1}	(N–N) cm^{-1}	(C–O) cm^{-1}	(C=O) cm^{-1}	(N–H) cm^{-1}	(Ni–N) cm^{-1}	(Ni–O) cm^{-1}	Bands due to heterocyclic base
L[1]	1612	–	1035	–	1720	3062	–	–	1445
1	1582	1530	1072	1290	–	3063	463	430	1442
2	1592	1536	1065	1271	1660	3358, 3288	485	445	1443
3	1598	–	1068	–	1667	3160, 3057	495	420	1447
4	1588	–	1070	–	1628	3332, 3358	460	422	1446

ligand [42]. The other band (~400 nm) may be due to ligand-to-metal charge-transfer transition. Complexes **1**, **2**, and **3** show three strong absorptions and a weak absorption [$^3A_{2g} \rightarrow {}^3T_{2g}$ (ν_1), $^3A_{2g} \rightarrow {}^3T_{1g}$ (F) (ν_2), $^3A_{2g} \rightarrow {}^3T_{1g}$ (P) (ν_3)], characteristic of regular octahedral nickel(II) complexes [43]; **4** does not show these bands separately.

3.5. *Molar conductivity*

The molar conductivities of **1**–**4** were measured in DMSO solution (3×10^{-3} mol L^{-1}). The molar conductivity (λ_m) values (110 $\Omega^{-1}cm^2mol^{-1}$ for **2**) indicate 1 : 1 electrolyte [42]. The values 249 and 262 $\Omega^{-1}cm^2mol^{-1}$ indicate the presence of 1 : 2 electrolyte [44] in **3** and **4**. However, for **1** $\lambda_m = 8$ $\Omega^{-1}cm^2mol^{-1}$ was obtained, which is significantly lower than the usual values for 1 : 1 electrolyte, suggesting the non-electrolytic behavior for **1** [44].

3.6. *Magnetic moment*

The magnetic susceptibilities of the nickel(II) complexes were determined in the solid state at room temperature. Nickel(II) ($3d^8$) should exhibit a magnetic moment higher than expected for two unpaired electrons in octahedral (2.8–3.2 B.M.) [45] and tetrahedral [3.4–4.2 B.M.] complexes whereas square-planar complexes would be diamagnetic. The room temperature effective magnetic moments (μ_{eff}) of **1**, **2**, **3**, and **4** were 2.89, 2.79, 2.83, and 2.91 B.M., respectively, consistent with octahedral geometry.

3.7. *IR spectroscopy*

Tentative assignments of significant IR spectral bands of L and its nickel complexes are presented in table 8. A high intensity band at 1610 cm^{-1} for L is from ν(C=N) [46], proof for the formation of Schiff base. A high intensity band at 1700–1730 cm^{-1} was assigned to ν(C=O). On coordination of the azomethine nitrogen ν(C=N_{azo}) shifts to lower wavenumbers by 10–20 cm^{-1} [47] from 1610 cm^{-1} in uncoordinated spectrum to ~1592 cm^{-1} in spectra of complexes. Coordination of the azomethine nitrogen is confirmed by a new band at 450–490 cm^{-1}, assigned to (Ni–N) [48]. The shifts in the (N–N) frequencies also support coordination through the azomethine nitrogen in the complexes. However in **3** and **4** broad bands are seen at 3415 cm^{-1} and 3440 cm^{-1} [49], respectively, due to the presence of lattice water. In the spectrum of **3**, there is also

Table 9. Cyclic voltammetric data for 1 mmol L^{-1} solution of the nickel(II) complexes in DMSO containing 0.1 mol L^{-1} $NaClO_4$ as supporting electrolyte.

Complex	Scan rate	E_{pc} (mV)	I_{pc} (μA)	E_{pa} (mV)	I_{pa} (μA)	ΔE_p (mV)	$E^{0'}$ (mV)	I_{pa}/I_{pc} (μA)
1	100	–1045	0.941	–995	0.679	50	–1020	0.721
	200	–1081	1.086	–971	0.724	110	–1026	0.666
	300	–1104	1.123	–952	0.868	152	–1028	0.773
2	100	–564	1.241	–428	0.496	135	–496	0.400
	200	–572	1.448	–389	0.675	182	–480	0.466
	300	–589	1.583	–376	0.837	212	–482	0.529
3	100	–1110	2.819	–1015	2.612	95	–1062	0.926
	200	–1119	4.184	–1006	3.871	113	–1062	0.925
	300	–1125	5.917	–1000	5.517	125	–1062	0.932
4	100	–849	3.165	–735	1.054	–114	–626	0.333
	200	–856	3.964	–729	1.266	–127	–630	0.319
	300	–864	4.439	–735	1.478	–129	–626	0.333

$\Delta E_p = E_{pa} - E_{pc}$; $E^{o\prime} = (E_{pa} + E_{pc})/2$.

a medium to high intensity band at 850 cm^{-1} assigned to coordinated water [50]. Some new bands with medium to weak intensities appear at 395–505 cm^{-1} in the complexes, which are assigned to (Ni–O/Ni–N) modes [51]. Coordination of the pyridine nitrogen is seen by shifts in frequencies of the deformation modes in the range 455–649 cm^{-1} in the spectrum of ligand [52]. This is further supported by ($Ni–N_{py}$) bands seen at ~250 cm^{-1} for all the complexes. In perchlorate complexes, the bands at ~1100 cm^{-1} and at 625 cm^{-1} indicate that T_d symmetry of ClO_4^- is maintained in complexes, suggesting ClO_4^- outside the coordination sphere in **2**–**4** [53]. A single sharp narrow band at 1750–1800 cm^{-1} is indicative of ionic nitrate [54] in **3**.

3.8. *Cyclic voltammetry*

Cyclic voltammograms of **1**–**4** were recorded in DMSO with sodium perchlorate as supporting electrolyte. The results are presented in table 9 and representative voltammogram of **4** is shown in "Supplementary material." All the complexes show similar electrochemical behavior. In the cyclic voltammograms of every complex for each scan rate two redox couples are observed; **3** and **4** show well-separated quasireversible redox couples whereas in **1**, one redox couple is not well-separated. Tabbi *et al.* [55] also reported that due to the width of the peak two redox steps cannot be detected but only one broad peak. Complex **2** shows only one redox couple in the voltammogram.

Analysis of the cyclic voltammograms of **4** indicates two well-separated redox couples. Both originate from a quasireversible process with peak-to-peak separation (ΔE_p) of 100–350 mV [55]. This complex shows one electron [56] quasireversible cyclic voltammetric response. In the voltammograms of **4**, the current values show two reduction peaks corresponding to Ni(II)/Ni(I) [57] and Ni(I)/Ni(0), the first at $E_{pc} = 0.625$ V with an associated oxidation peak at $E_{pa} = 0.880$ V and the second reduction at $E_{pc} = -0.856$ V with an associated oxidation peak at $E_{pa} = -0.729$ V. The values of ΔE_p are 255 and –127 for first and second redox couples, respectively.

Table 10. Antibacterial activity of L and **1–4**.

Complex	Conc. ($\mu g\,mL^{-1}$)	Diameter of inhibition zone (in mm) *E. coli*
L	10	6
	15	8
	20	9
1	10	8
	15	10
	20	13
2	10	7
	15	10
	20	12
3	10	9
	15	11
	20	13
4	10	8
	15	9
	20	11
DMSO (Control)		Nil

The peak current ratio I_{pa}/I_{pc} less than unity shows that the electron transfer reaction is followed by a chemical reaction (EC mechanism) [58].

3.9. *Antibacterial activity*

Complexes **1–4** were evaluated against *Escherichia coli* bacteria as the test organism in an antimicrobial study. Antibacterial assessments of the complexes were tested as a function of concentration. The susceptibility of bacteria toward the present nickel(II) complexes were determined by measuring the size of inhibition diameter. Growth inhibitory effects were observed against *E. coli*, which causes dysentery and food poisoning. Complexes **1–4** are moderately active against *E. coli* (Supplementary material). The activity was also assayed for pure DMSO. The zone of inhibition in mm for the ligand and nickel(II) complexes are presented in table 10. The metal chelates exhibit higher antimicrobial activities than free ligand. Similar antimicrobial results were reported in the literature [59–63] on simple nickel(II) binary and ternary complexes. Ligand and metal complexes are moderately active toward bacterial cells. Thus, it can be concluded that these complexes may serve as bactericides.

3.10. *SOD activity*

The SOD activities for the present complexes were measured. The concentration causing 50% inhibition of NBT reduction is IC_{50}. The observed IC_{50} values of the complexes were compared with earlier reported values for nickel(II) complexes [64]. The catalytic activity of NiSOD [65], however, is on the same high level as that of Cu–ZnSOD at about $10^9\,(mol\ L^{-1})^{-1}s^{-1}$ per metal center. The IC_{50} data of the SOD activity assay along with kinetic catalytic constants of **1–4** [66, 67] are presented

Table 11. IC_{50} values and kinetic constant of **1–4**.

Complex	IC_{50} (μmol)	k_{McCF} $((mol\ L^{-1})^{-1}s^{-1}) \times 10^4$	Reference
$[Ni(L)_2]$	31	3.06	This work
$[Ni(L)(HL)](ClO_4)(H_2O)$	54	1.76	This work
$[Ni(HL)(bipy)(H_2O)](NO_3)(ClO_4)(H_2O)$	38	2.5	This work
$[Ni(HL)(dien)](ClO_4)_2(H_2O)$	95	1.0	This work
$[Ni(L^1)_2]2H_2O$	35	2.71	[64]
$[Ni(L^2)_2](ClO_4)_2$	55	1.73	[64]
$[Ni(L^3)(bipy)](ClO_4)_2$	60	1.58	[64]

k_{McCF} were calculated by $K = k_{NBT} \times [NBT]/IC_{50}$, k_{NBT} (pH 7.8) $= 5.94 \times 10^4$ $(mol\ L^{-1})^{-1}s^{-1}$ [67].

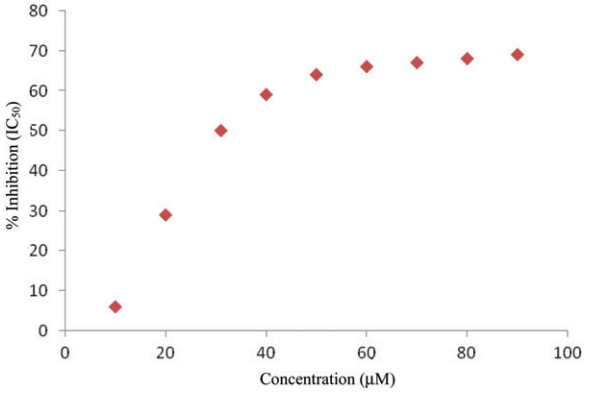

Figure 5. SOD activity of **1**.

in table 11 and a representative inhibition curve for **3** is shown in figure 5. Complex **1** shows highest SOD activity ($IC_{50} = 31$ μmol dm^{-3}) whereas other three show $IC_{50} = 54$, 38, and 95 μmol dm^{-3} for **2**, **3**, and **4**.

4. Conclusion

We report the syntheses and crystal structures of four mononuclear nickel(II) complexes. The carbonyl in the Schiff base provides an anchor to form two distinguishable hydrogen-bonded motifs in all the complexes. The Schiff base contains three different ligating atoms in one molecule. We also report biological activity of the complexes. Crystal packing of each complex is affected by intermolecular and intramolecular hydrogen bonds. Analytic, spectroscopic, magnetic, electrochemical, and crystal structure determinations show that nickel(II) has octahedral geometry.

Supplementary material

CCDC 768579, 768578, 768577, and 768576 contain the supplementary crystallographic data for $[Ni(L)_2]$ (**1**), $[Ni(L)(HL)](ClO_4)(H_2O)$ (**2**), $[Ni(HL)(bipy)(H_2O)](NO_3)$

$(ClO_4)(H_2O)$ (**3**), and $[Ni(HL)(dien)](ClO_4)_2(H_2O)$ (**4**) and have been synthesized with Schiff base derived from 2-pyridinecarboxaldehyde and benzoylhydrazine, where L = N-[(1)-pyridin-2-ylmethylidene]benzohydrazide. These data can be obtained free of charge *via* http://www.ccdc.cam.ac.uk/conts/retrieving.html, or from the Cambridge Crystallographic Data Centre, 12 Union Road, Cambridge CB2 1EZ, UK; Fax: (+44) 1223-336-033; or E-mail: deposit@ccdc.cam.ac.uk.

Acknowledgments

Our grateful thanks are due to the National Diffraction Facility, X-ray Division, and RSIC (SAIF), IIT Mumbai for single-crystal data collection and EPR measurements, respectively. The Head RSIC (SAIF), Central Drug Research Institute, Lucknow is also gratefully acknowledged for providing analytical and spectral facilities. Financial assistance from UGC [Scheme no. 36–28/2008 (SR)] and CSIR [Scheme no. 01(2451)/11/EMR-II] New Delhi are also gratefully acknowledged.

References

[1] J.A. McCleverty, T.J. Meyer (Eds). *Comprehensive Coordination Chemistry II: From Biology to Nanotechonology*, Vol. 1, p. 447, Elsevier, Pergamon, Oxford (2004).
[2] A. Mederos, S. Dominguez, R. Hernandez-Molina, J. Sanchiz, F. Brito. *Coord. Chem. Rev.*, **193**, 857 (1999).
[3] D.M. Boghaei, S. Mohebi. *Tetrahedron*, **58**, 5357 (2002).
[4] R. Klement, F. Stock, H. Elias, H. Paulus, P. Pelikan, M. Valko, M. Mazur. *Polyhedron*, **18**, 3617 (1999).
[5] J.W. Steed, J.L. Atwood. *Supramolecular Chemistry*, Wiley, New York (2000).
[6] B. Moulton, M.J. Zaworotko. *Chem. Rev.*, **101**, 1629 (2001).
[7] M.J. Zaworotko. *Chem. Commun.*, 1 (2001).
[8] J.K.A. Howard, F.H. Allen (Eds). *Implications of Molecular and Materials Structure for New Technologies*, Kluwer, Dordrecht (1999).
[9] D. Bose, J. Benerjee, S.H. Rahaman, G. Mostafa, H.-K. Fun, R.D.B. Walsh, M.J. Zaworotko, B.K. Ghosh. *Polyhedron*, **23**, 2045 (2004).
[10] T. Steiner. *Angew. Chem. Int. Ed.*, **41**, 48 (2002).
[11] G.R. Desiraju. *Acc. Chem. Res.*, **35**, 565 (2002).
[12] M.J. Zaworotko. *Chem. Commun.*, 199 (2002).
[13] C. Abernethy, C.L.B. Macdonald, J.A.C. Clyburne, A.H. Cowley. *Chem. Commun.*, 61 (2001).
[14] L. Rong-Guang, T. Zhu, X. Sai-Feng, Z. Quin-Jiang, W.G. Jackson, W. Zhan-Bing, L. La-Sheng. *Polyhedron*, **22**, 3467 (2003).
[15] G.W. Gokel, A. Mukhopadhyay. *Chem. Soc. Rev.*, **30**, 274 (2001).
[16] O.R. Evans, W. Lin. *Acc. Chem. Res.*, **35**, 511 (2002).
[17] J.S. Miller, M. Drilon (Eds). *Magnetism: Molecules to Materials*, Vol. 3, Wiley-VCH, Weinheim (2002).
[18] B. Cornils, W.A. Herrmann, R. Schlogl, W.-H. Wong (Eds). *Catalysis from A to Z: A Concise Encyclopedia*, Wiley-VCH, Weinheim (2000).
[19] M. Kondo, T. Yoshitomi, K. Seki, H. Matsuzaka, S. Kitagawa. *Angew. Chem., Int. Ed. Engl.*, **36**, 1725 (1997).
[20] T.K. Karmakar, S.K. Chandra, J. Ribas, G. Mostafa, T.-H. Lu, B.K. Ghosh. *Chem. Commun.*, 2364 (2002).
[21] S. Konar, E. Zangrando, M.G.B. Drew, T. Mallah, J. Ribas, N.R. Choudhary. *Inorg. Chem.*, **42**, 5966 (2003).
[22] D. Bose, S.H. Rahaman, G. Mostafa, R.D. Bailey Walsh, M.J. Zaworotko, B.K. Ghosh. *Polyhedron*, **23**, 545 (2004).
[23] D. Bose, G. Mostafa, H.-K. Fun, B.K. Ghosh. *Polyhedron*, **24**, **747** (2005).
[24] P. Comba, T.W. Hambley. *Molecular Modelling of Inorganic Compounds*, 2nd Edn, Wiley-VCH, Weinheim (2001).

[25] A. Camus, N. Marsich, A.M.M. Lanfredi, F. Ugozzoli, C. Massera. *Inorg. Chim Acta*, **309**, 1 (2000).
[26] F.A. Cotton, L.M. Daniels, G.T. Jordan IV, C.A. Murillo. *J. Am. Chem. Soc.*, **119**, 10377 (1997).
[27] M. Villanueva, J.L. Mesa, M.K. Urtiga, R. Cortes, L. Lezama, M.I. Arriortua, T. Rojo. *Eur. J. Inorg. Chem.*, 1581 (2001).
[28] L.P. Wu, P. Field, T. Morrissey, C. Murphy, P. Nagle, B.J. Hathaway, C. Simmons, P. Thornton. *J. Chem. Soc., Dalton Trans.*, 3835 (1990).
[29] W. Liu, A. Hassan, S. Wang. *Organometallics*, **16**, 4257 (1997).
[30] B. Barszcz. *Coord. Chem. Rev.*, **249**, 2259 (2005).
[31] R.G. Bhirud, T.S. Srivastava. *Inorg. Chim. Acta*, **179**, 125 (1991).
[32] H.B. Gray, J. Ballhausen. *J. Am. Chem. Soc.*, **85**, 260 (1963).
[33] G.M. Sheldrick. *SHELXS-97, Program for the Solution for Crystal Structures*, University of Göttingen, Göttingen, Germany (1997); *Acta Crystallogr., Sect. A*, **64**, 112 (2008).
[34] G.M. Sheldrick. *SHELXL-97, Program for the Refinement of Crystal Structures*, University of Göttingen, Göttingen, Germany (1997).
[35] I. Garcia, E. Bermejo, A.K. EI-Sawaf, A. Castineiras, D.X. West. *Polyhedron*, **21**, 729 (2002).
[36] Y.B. Dong, M.D. Smith, H.C. zur Loye. *Solid State Sci.*, **2**, 335 (2000).
[37] M.M. Morelock, M.L. Good, L.M. Trefonas, D. Karraker, L. Maleki, H.R. Eichelberger, R. Majesti, J. Dodge. *J. Am. Chem. Soc.*, **101**, 4858 (1979).
[38] J. March. *Advanced Organic Chemistry, Reactions Mechanisms and Structure*, 4th Edn, Wiley, New York (1992).
[39] A.T. Chaviara, P.J. Cox, K.H. Repana, A.A. Pantazaki, K.T. Papazisis, A.H. Kortsaris, D.A. Kyriakidis, G.S. Nikolov, C.A. Bolos. *J. Inorg. Biochem.*, **99**, 467 (2005).
[40] G.A. van Albada, I. Dominicus, I. Mutikainen, U. Turpeinen, J. Reedijk. *Polyhedron*, **26**, 3731 (2007).
[41] A. Sreekanth, S. Sivakumar, M.R.P. Kurup. *J. Mol. Struct.*, **655**, 47 (2003).
[42] H. Beraldo, W.F. Nacif, L.R. Teixeira, J.S. Reboucas. *Transition Met. Chem.*, **27**, 85 (2002).
[43] S. Jena, R.N. Nath, K.C. Dash. *Indian J. Chem.*, **38A**, 350 (1999).
[44] W.J. Geary. *Coord. Chem. Rev.*, **7**, 81 (1971).
[45] X.Y. Le, M.L. Tang. *J. Inorg. Chem.*, **18**, 1023 (2002).
[46] S.H. Abo, E. Fetoh, A.E. Eid, A.E. Abd, E. Kareem, M.A. Wassel. *Synth. React. Inorg. Met.-Org. Chem.*, **30**, 513 (2000).
[47] G.R. Burns. *Inorg. Chem.*, **7**, 277 (1968).
[48] P. Souza, J.A. Garcia-Vazquez, J.R. Masaguer. *Transition Met. Chem.*, **9**, 318 (1984).
[49] E. Manoj, M.R.P. Kurup. *Polyhedron*, **27**, 275 (2008).
[50] M.A. Phaniband, S.D. Dhumwad. *J. Coord. Chem.*, **62**, 2399 (2009).
[51] K. Nakamoto. *Infrared Spectra of Inorganic and Coordination Compounds*, 2nd Edn, Wiley-Interscience, New York (1970).
[52] A. Sreekanth, M.R.P. Kurup. *Polyhedron*, **22**, 3321 (2003).
[53] M. Akbar Ali, S.M.G. Hossain, S.M.M.H. Majumder, M. Nazimuddin, M.T.H. Tazafder. *Polyhedron*, **6**, 1653 (1987).
[54] A.B.P. Lever, E. Mantovani, B.S. Ramaswamy. *Can. J. Chem.*, **49**, 1957 (1971).
[55] G. Tabbi, W.L. Driessen, J. Reedijk, R.P. Bonomo, N. Veldman, A.L. Spek. *Inorg. Chem.*, **36**, 1168 (1997).
[56] N. Raman, S. Ravichandran, C. Thangaraja. *J. Chem. Sci.*, **116**, 215 (2004).
[57] A.K. Patra, R. Mukherjee. *Inorg. Chem.*, **38**, 1388 (1999).
[58] D.H. Evans. *Chem. Rev.*, **90**, 739 (1990).
[59] M.T.H. Tarafder, K.B. Chew, K.A. Crouse, A.M. Ali, B.M. Yamin, H.K. Fun. *Polyhedron*, **21**, 2683 (2002).
[60] M. Kalanithi, M. Rajarajan, P. Tharmaraja. *J. Coord. Chem.*, **64**, 842 (2011).
[61] S.G. Shankarwar, T.K. Chandhekar. *J. Coord. Chem.*, **63**, 4153 (2010).
[62] D. Arish, M.S. Nair. *J. Coord. Chem.*, **63**, 1619 (2010).
[63] N. Singh, K.K. Shukla, R.N. Patel, U.K. Chauhan, R. Shrivastava. *Spectrochim. Acta*, **A59**, 3111 (2003).
[64] R.N. Patel, K.K. Shukla, Anurag Singh, M. Choudhary, D.K. Patel, J. Niclós-Gutiérrez, D. Choquesillo-Lazarte. *J. Coord. Chem.*, **63**, 3648 (2010).
[65] H.D. Youn, E.J. Kim, J.H. Roe, Y.C. Hah, S.O. Kang. *Biochem. J.*, **318**, 889 (1996).
[66] Z.-R. Liao, X.-F. Zheng, B.-S. Luo, L.-R. Shen, D.-F. Li, H.-L. Liu, W. Zhao. *Polyhedron*, **20**, 2813 (2001).
[67] R.F. Pasternock, B. Halliwell. *J. Am. Chem. Soc.*, **101**, 1026 (1979).